Biochemical and Biophysical Research Communications 386 (2009) 159–164

Contents lists available at ScienceDirect

Biochemical and Biophysical Research Communications

journal homepage: www.elsevier.com/locate/ybbrc

Structural basis of the autolysis of AaHIV suggests a novel target recognizing model for ADAM/reprolysin family proteins

Zhiqiang Zhu, Yongxiang Gao, Zhongliang Zhu, Yang Yu, Xiao Zhang, Jianye Zang, Maikun Teng *, Liwen Niu *

Hefei National Laboratory for Physical Sciences at Microscale and School of Life Sciences, University of Science and Technology of China, Hefei, Anhui 230026, China
Key Laboratory of Structural Biology, Chinese Academy of Sciences, Hefei, Anhui 230026, China

ARTICLE INFO

Article history:
Received 28 May 2009
Available online 6 June 2009

Keywords:
Metalloproteinase
Cysteine-rich
Disintegrin-like
Autodegradation

ABSTRACT

AaHIV, a P-III-type snake venom metalloproteinase (SVMP), consists of metalloproteinase/disintegrin/cysteine-rich (MDC) domains and is homologous to a disintegrin and metalloproteinase (ADAM) family proteins. Similar to brevilysin H6 and jararhagin, AaHIV can easily autolyse to release a stable protein named acucetin, which contains disintegrin-like and cysteine-rich domains. In this study, we determined the crystal structure of AaHIV and investigated the autolysis mechanism. Based on the structure of AaHIV and the results from docking experiments, we present a new model for target recognition in which two protein molecules form a functional unit, and the DC domain of one molecule is used for target recognition while the M-domain of the other is used for target proteolysis. Our results shed new light on the mechanism of target recognition and processing in ADAM/reprolysin family proteins.

Introduction

Snake venom, which is very toxic, is a mixture of proteins and peptides with different biological activities. Snake venom metalloproteinases (SVMPs) act synergistically with many other toxins to cause severe bleeding [1]. SVMPs are members of the reprolysin subfamily of the M12 family of metalloproteinases [2], and based on their domain organization, they are classified as P-I, P-II, P-III, and P-IV [3]. P-III-type SVMPs possess a metalloproteinase domain (M-domain), a disintegrin-like domain (D-domain), and a cysteine-rich domain (C-domain). P-IV-type SVMPs have an additional C-lectin domain linked to the other domains through a disulfide bond. The P-III-type and P-IV-type SVMPs are grouped into the ADAM/reprolysin family of proteins on the basis of their MDC domain architecture [2].

It has been found that some P-III-type SVMPs, including brevilysin H6 [4], jararhagin [5], and bothropasin [6], can be degraded through autoproteolytic events *in vitro*. This degradation process leads to the release of a stable fragment consisting of a disintegrin-like domain and a cysteine-rich domain. During the autoproteolysis of brevilysin H6, more than 25 peptide bonds may be cleaved, C-terminal to which are some hydrophobic amino acid residues [4]. Based on the autodegradation feature mentioned above, these metalloproteinases are classified in the P-IIIb subfamily [5].

The widely accepted mechanism for the hemorrhagic activity of SVMPs is one in which these metalloproteinases degrade the capillary basement membranes and surrounding extracellular matrix thereby promote bleeding from capillaries [7]. Moreover, SVMPs also degrade blood coagulation proteins such as fibrinogen and the von Willebrand factor (VWF) [8]. Similarly, ADAMs, which constitute a family of mammalian membrane-anchored glycoproteins, are implicated in the processing of cell surface and extracellular matrix proteins [9,10]. To date, the structure of an intact ADAM with all its MDC domains has not been determined, and the structural basis of the catalytic and adhesive functions of this family of proteins is elusive. Recently, the crystal structures of VAP1, VAP2B and bothropasin, which belong to the P-III SVMP family, were reported [11–13]. However, there are few studies on the autolytic mechanism of P-IIIb subfamily proteins and the function of the D-domain in target recognition.

AaHIV is a P-III-type metalloproteinase from *Agkistrodon acutus* venom. It is an acidic protein with strong caseinolytic activity at pH 7–9 and can induce hypodermic hemorrhage [14]. This protein can be autodegraded to a stable fragment named acucetin containing the DC domain [15]. In this study, we present the crystal structure of AaHIV. Based on this, we examine the autolytic mechanism of this protein. The autolytic process suggests a novel model of target recognition by ADAM/reprolysin family proteins.

Materials and methods

Purification of AaHIV and an intermediate. AaHIV from *A. acutus* venom was purified using a previously described procedure [14]. A high molecular weight intermediate of AaHIV-to-acucetin was obtained from the autolysis solution of AaHIV by using one-step li-

* Corresponding authors. Fax: +86 551 3606314 (M. Teng).
E-mail addresses: mkteng@ustc.edu.cn (M. Teng), lwniu@ustc.edu.cn (L. Niu).

0006-291X/$ - see front matter © 2009 Elsevier Inc. All rights reserved.
doi:10.1016/j.bbrc.2009.06.004

quid chromatography, and the resulting protein was sequenced (details provided in Supplementary material).

Autolysis assay of AaHIV. AaHIV dissolved in 0.1 M Tris–HCl buffer (1 mg/ml, pH 8.0) was incubated at 37 °C for different time intervals or under other conditions in the presence of EDTA, PMSF, Ca^{2+}, or $HgCl_2$. The reaction was terminated by adding SDS–PAGE loading buffer containing 0.2 M β-mercaptoethanol. SDS–PAGE (12%) was performed under reducing conditions to examine the products of autoproteolysis. The effects of changing the reaction pH values and lowering the temperature on autoproteolysis were also analyzed by SDS–PAGE.

Crosslinking assay. Crosslinking experiments were carried out to identify the functional unit. Several AaHIV solutions at a concentration of 1 mg/ml in 20 mM phosphate buffer (pH 7.5) were incubated at room temperature with different molar excesses of BS^3. After 1.5 h, the reaction was quenched by adding Tris–HCl buffer to a final concentration of 50 mM, and the products were examined by 10% SDS–PAGE under nonreducing conditions.

Protein crystallization and structure determination. A single crystal of AaHIV was obtained by the hanging-drop vapor diffusion method. The diffraction data set was collected and processed, and the crystal structure of AaHIV was solved and refined. Details are provided in Supplementary material. Some quality parameters are also summarized in Table s1. The atomic coordinates were deposited in the Protein Data Bank (3HDB).

Results and discussion

Autolysis and sequence analysis of AaHIV

AaHIV could autolyse and release a stable protein product named acucetin [15]. SDS–PAGE revealed that acucetin appeared soon after the autoproteolytic reaction was initiated at 37 °C, and little AaHIV remained after incubation for 20 h at pH 8.0 and 37 °C (Fig. 1A). A relatively high concentration (5 mM) of EDTA, which is an effective inhibitor of metalloproteinases, could significantly disrupt the proteolysis (Fig. 1A). Both 5 mM PMSF and 0.1 mM $HgCl_2$ (which are inhibitors of serine proteases and thiol proteases, respectively) had little effect on the autodegradation of AaHIV (Fig. 1A), indicating that the proteolysis was actually performed by AaHIV itself. This was consistent with the observations from other studies on P-III-type SVMPs [4–6]. Similar to its caseinolytic activity [14], the rate of autodegradation could be significantly reduced even at 37 °C by lowering the pH of the reaction system (e.g., by reducing it to pH 4.0, Fig. 1B). Apart from the pH, changes in other conditions, for example, adding 10 mM Ca^{2+} or 1 mM EDTA or reducing the temperature, could also decrease the autoproteolysis rate of AaHIV (Fig. 1C). At the same time, a high molecular weight band (approximately 100 kDa) was detected (Fig. 1C). This indicated the presence of some dimers during the course of AaHIV autolysis. It was difficult to disrupt these dimers using a low concentration of SDS, as in the case of the dimer formed between fertilin α and β [16].

Under weakly acidic conditions, an intermediate of approximate molecular weight 43 kDa could be purified, and the sequence of N-terminal amino acid residues was found to be L(277)LAEKKHDNAQLITGIDFRGSIIGYAYIGS. This proved that the intermediate was a single-chain peptide. In addition, the amino acid sequences of three fragments of acucetin were reported to be LYCKDDSPGQNNPCKMFYS, MFYSNDDEHKGMVLPGTK, and LGTDIISPPLCGNELLEVGEECDCGTPENCQ [15]. These four amino acid sequences of AaHIV fragments are identical to the sequence of acutolysin E (GenBank: AAD27891.1). Therefore, the sequence of acutolysin E was used as the reference sequence during structure determination.

Dimerization of AaHIV

After crosslinking, a new band of approximate size 100 kDa, which corresponded to the AaHIV dimer, appeared on SDS–PAGE (Fig. 1D). The amount of dimers increased as the crosslinker to AaHIV molar ratio increased. When the molar ratio reached 400, many AaHIV molecules still existed as monomers. Thus, only some AaHIV molecules were present as dimers.

Overall structure of AaHIV

In the crystal structure of AaHIV, one molecule in the crystal has a large interface with its neighboring molecule, indicating that AaHIV may form dimers under some conditions. A similar crystal packing pattern has also been observed in the crystal structures of bothropasin and VAP2B [12,13]. When the dimers of these three proteins are superimposed, only small differences are observed (Fig. 3A).

Similar to VAP2B, bothropasin, and VAP1, the crystal structure of AaHIV also reveals the presence of the M-, D-, and C-domains [12–14]. The overall structure is shown in Fig. s1A. The structure of the first domain is very similar to the corresponding structures of acutolysin A [17] and ADAM33 [18]; it forms a flat ellipse with a core of a five-stranded β-sheet surrounded by four α-helices (Fig. s1A). It contains the conserved HEXXHXXGXXHD sequence, including three histidines (His333, His337, and His343) that function as ligands of the catalytic zinc ion and a conserved methionine (Met357, Met-turn) that is present downstream of the zinc-binding sequence (Fig. 2). These are typical structural features of the metzincin family of metalloproteinases [19]. A bound calcium ion (Ca^{2+}-binding site I) has been identified as in the structures of acutolysin A [17] and ADAM33 [18] (Figs. 2, s1A). The DC domain forms a curved structure with the concave surface toward the M-domain. This stretches the distal portion of the C-domain close to the catalytic site, and the entire molecule thus adopts a C-shaped conformation. The structure of the DC domain is stabilized by 14 disulfide bonds and 2 additional calcium ions (sites II and III) (Figs. 2 and s1A). Sequence alignment of some ADAM/reprolysin family proteins shows the presence of a highly divergent and variable region containing residues 561–582 of the Ch domain (Fig. 2); this is in the distal portion of the C-shape and has been designated as the hypervariable region (HVR) in the VAP1 and VAP2B structures [11,12]. A conserved cysteine residue in this region forms a disulfide bond that divides the HVR into HVR1 and HVR2 (Fig. 2), which may have different functions (discussed below). The location of the cysteine residues and the Ca^{2+}-binding sites are conserved among ADAM/reprolysin family proteins (Fig. 2).

Environment of the catalytic site of the M-domain and the HVR of the C-domain

To explore the structural basis of the catalytic mechanism of SVMPs, some tripeptide inhibitors were co-crystallized with TM-3 from the *Taiwan habu* venom, and the structures of the complexes (1kug, 1kui, and 1kuk) were determined [20]. The structure of metalloproteinase FII from Anhui *A. acutus* snake venom is the only reported structure of a natural complex of a SVMP with its peptide inhibitor [21]. In the AaHIV structure, there is a tripeptide (KNL) in the catalytic site that forms five hydrogen bonds with the main chain atoms of the M-domain and coordinates with the zinc ion at the enzyme's active site (Fig. 3B). The tripeptide may mimic the cleavage site of target proteins.

The HVR of the cysteine-rich domain participates in the interaction between two neighboring AaHIV molecules, which exhibit a packing pattern similar to that found in VAP2B and bothropasin [12,13] (Fig. 3A). The Tyr575-Asn577 stretch in the HVR2 of both

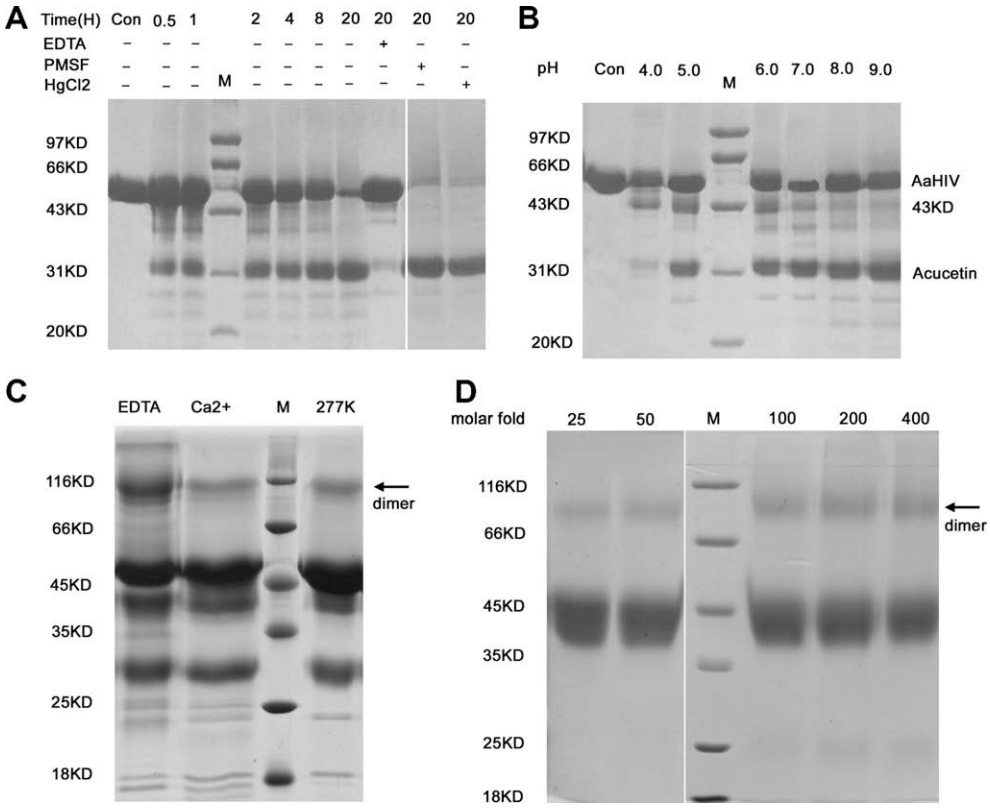

Fig. 1. SDS–PAGE analysis of the autolysis and dimerization of AaHIV. (A) AaHIV was incubated for different time intervals (0–20 h) at 37 °C in the absence or presence of 5 mM EDTA, 0.1 mM $HgCl_2$, or 5 mM PMSF. (B) AaHIV was incubated for 4 h at 37 °C under different pH conditions. (C) AaHIV was incubated for 2 h at 4 °C or 37 °C in the presence of 1 mM EDTA or 10 mM Ca^{2+}. (D) Different molar ratios of BS^3 relative to AaHIV were used in the crosslinking assay. Control (lane Con in A and B): AaHIV; lane M, protein marker. The symbols + and − represent the presence and absence of the indicated compounds.

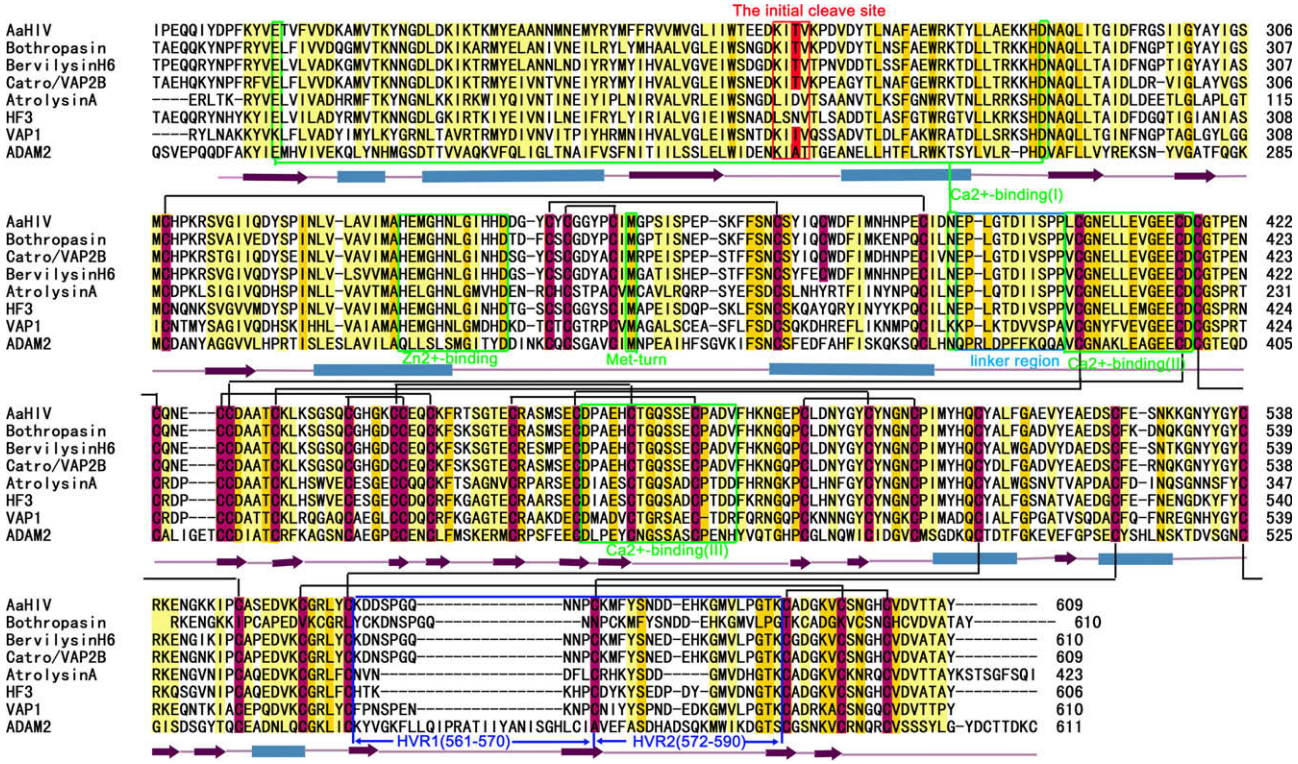

Fig. 2. Sequence alignment of AaHIV with other SVMPS and ADAM2. The cysteine residues and conserved residues are shaded in purple and yellow, respectively. The Ca^{2+}-binding sites, Zn^{2+}-binding site, and MET turn are boxed in green; HVR1 and HVR2 are boxed in blue; and the initial cleavage site is boxed in red. Secondary structures are drawn schematically. Disulfide bond formation is shown by a black line that connects the corresponding partners. Atrolysin A, HF3, and VAP1 cannot autolyze; the first two belong to the P-IIIa SVMP family, while the third belongs to the P-IIIc family [8]. (For interpretation of the references to colour in this figure legend, the reader is referred to the web version of this paper.)

molecules (A and B) forms four symmetric hydrogen bonds (Fig. 3D), and residues Ser564-Asp568 in the HVR1 of molecule A interact with the residues close to the catalytic site of the M-domain of molecule B (Fig. 3C). Moreover, the Tyr507-Tyr519 stretch adjacent to the HVR1 of molecule A forms an additional interaction with molecule B close to the catalytic site (Fig. 3C). The interface between molecule A and molecule B calculated by PROTORP shows that the dimer in solution may prefer to adopt this interaction pattern. The HVR1 of molecule A is close to the catalytic site of B and may serve as a target recognition platform together with the residues that surround the catalytic site of molecule B.

Architectural flexibility

When the monomer structures of VAP1 (*2ero*), VAP2B (*2dw0*), and bothropasin (*3sdl*) are superimposed on that of AaHIV, the rmsds of the C_α atoms are found to be 5.68, 1.67, and 1.03 Å, respectively. Structural alignment of the M-domains of the three proteins with AaHIV over the C_α atoms yields rmsds of 0.81, 0.43, and 0.48 Å, respectively (Fig. S1B). The rmsds over the C_α atoms corresponding to the D-domain are 1.04, 0.44, and 0.37 Å, respectively, and the corresponding values over the C-domain are 0.46, 0.34, and 0.45 Å, respectively (Fig. s1C). This indicates that the linker regions between the domains are flexible, resulting in different orientations of these domains in these protein structures. When the metalloproteinase domains of VAP1, VAP2B, bothropasin, and AaHIV are superimposed, the DC domains rotate relative to the M-domain (Fig. s1C). Therefore, the linker between the M and DC domains may restrict the mobility of the shoulder joint and thus determine the preferred orientation of the M-domain relative to the rest of the molecule for the desired target. In comparison with the SVMPs, the linker regions of ADAMs show greater variability with different numbers of amino acids and more polar residues (Fig. s2). Based on this structure, we propose a similar model mentioned by Igarashi et al. [12], in which ADAMs and P-III SVMPs adhere to their target molecules through the cysteine-rich domains and cleave the targets with the metalloproteinase domains (Fig. 4B).

Initial site of autolysis

The crystal structure of AaHIV provides some information on the structural basis of the autolytic process. To identify the initial site of AaHIV autolysis, a protein intermediate of approximate molecular mass 43 kDa was purified and subjected to N-terminal amino acid sequencing. We speculated that the initial proteolysis site during autolysis must lie before or exactly at Leu277. Considering the possible interactions between the enzyme and target, the first cleavage site must be in the loop region and should be accessible to the enzyme. Another important factor is the sequence specificity of the enzyme. SVMPs prefer to recognize sites before hydrophobic amino acids and cleave peptide bonds that are N-terminal to hydrophobic amino acids, as proven by proteolytic experiments with brevilysin H6 [4]. Therefore, the hydrophobic amino acids in the loop regions on the surface of AaHIV before residue Leu277 were examined (Fig. 2). Based on the structure of AaHIV,

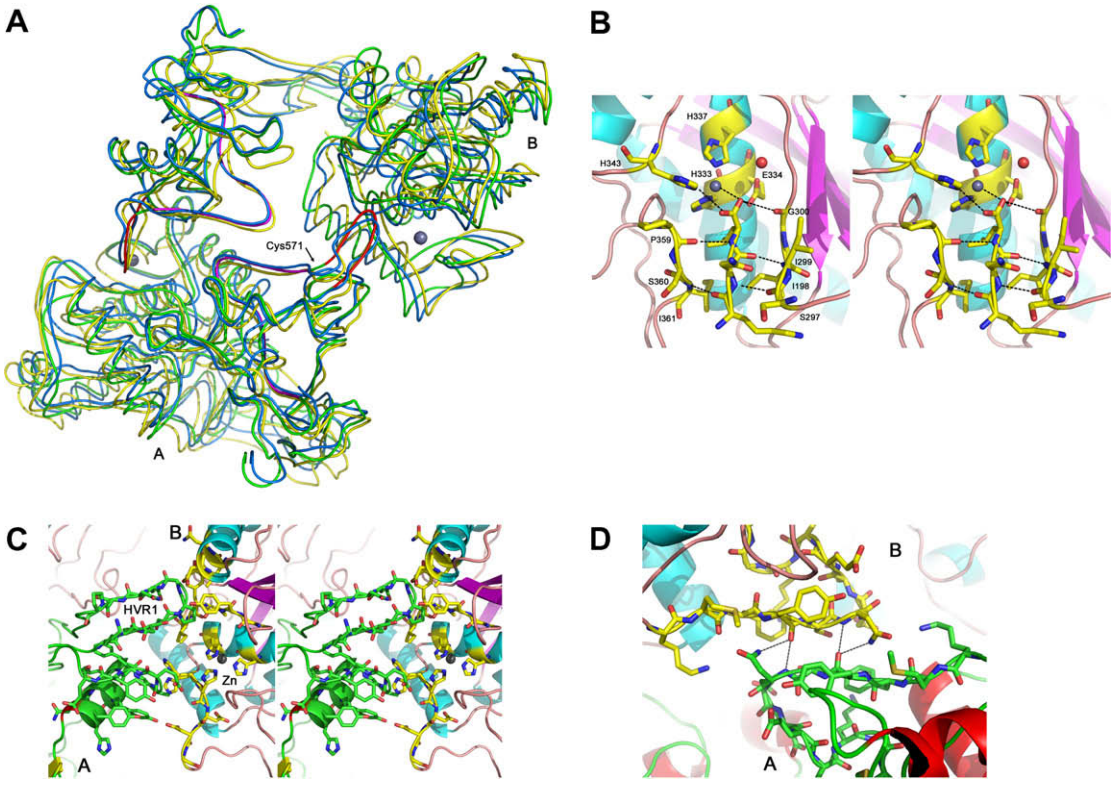

Fig. 3. Crystal packing of AaHIV molecules, stereoview of the structure of the catalytic site in AaHIV, and structure of the residues involved in AaHIV dimerization. (A) Structural superpositioning of bothropasin (*3sdl*, yellow), Catro/VAP2B (*2dw0*, blue), and AaHIV (green) presents a similar crystal packing pattern. The cysteine residue between HVR1 (red) and HVR2 (purple) is indicated, and the zinc ion at the catalytic site is shown in grey. (B) The tripeptide (KNL) stabilized by residues Pro359, Ser360, Ile361, Ser297, Ile298, Ile299, and Gly300 and the three histidines coordinated with the zinc ion are shown as sticks with the carbon atoms colored yellow. The zinc ion and a water molecule are colored grey and red, respectively. The hydrogen bonds between KNL and AaHIV are shown by dashed black lines. (C) The residue in HVR1, those close to HVR1, and the residues of molecule B involved in dimerization are represented as sticks. The zinc ion and its coordinating residues are also presented. (D) The residues involved in hydrogen bond formation in both HVR2s of molecules A and B are shown as sticks. The carbon atoms of the residues involved in the dimerization between molecules A and B are colored green and yellow, respectively. The zinc ion is in grey. (For interpretation of the references to colour in this figure legend, the reader is referred to the web version of this paper.)

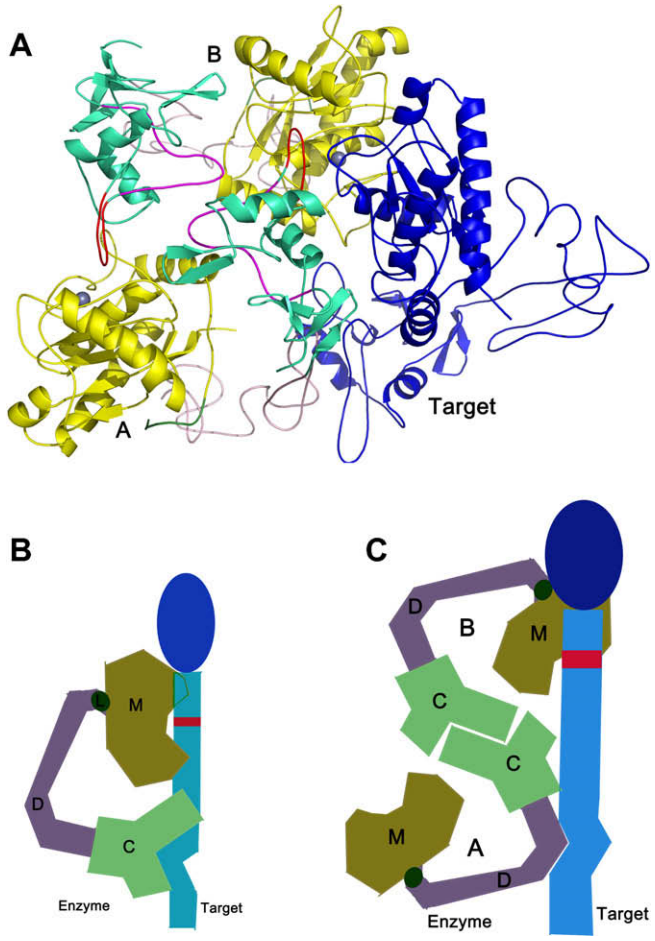

Fig. 4. The docking model of AaHIV and two models of target recognition and proteolysis by ADAM/reprolysin proteins. (A) The AaHIV dimer formed by molecules A and B interacts with a target monomer. The M, D, and C domains and the MD linker of molecules A and B are colored yellow, light pink, green, cyan and forest, respectively. HVR1, HVR2, and zinc ion are colored red, magenta, and grey, respectively. The monomer is colored blue. (B) The first model of target recognition and proteolysis by ADAM/reprolysin proteins in which these enzymes interact with their targets as monomers. (C) The second model in which these enzymes interact with their targets as dimers. The MDC domains of the enzyme are labeled and colored differently. The cleavage site of the target molecule is colored red. (For interpretation of the references to colour in this figure legend, the reader is referred to the web version of this paper.)

the accessibility of each amino acid residue before Leu277 was calculated (using program ASC1.3), and a single site at Lys255-Ile256-Thr257-Val258 was found to satisfy the conditions mentioned above. Sequence alignment of P-III SVMPs showed that the amino acid residue at site 257 varies in proteins that undergo autolysis and those that do not (Fig. 2). Thus, it is believed that the initial site of P-IIIb SVMPs autolysis lies between residues 255–258. Interestingly, ADAM2 is processed to mature fertilin-β by the loss of its pro-domain and metalloproteinase domain similar to the autolytic process of AaHIV, with hydrophobic amino acid residues C-terminal to the cleavage site (Fig. 2) [16]. ADAM2 may be cleaved by an ADAM family protein by a mechanism similar to that involved in the autodegradation of P-IIIb SVMP family proteins.

Mechanism of AaHIV autolysis and a new model for the process

By identifying the initial enzymatic cleavage site, some docking experiments were carried out based on the structure of the tripeptide in the catalytic site. The DC domain is another important restraining factor in docking because the autolytic process only occurs in P-IIIb SVMPs. The docking results showed that if autolysis occurs at the initial site between two monomers there is no interaction in the DC domain between the molecules. Some dimers do exist when autolysis occurs at a low temperature or at low EDTA or calcium ion concentrations, as shown by the results of the cross-linking assay. Therefore, autolysis may occur between one dimer and one monomer or between two dimers. When two dimers are docked, there is steric hindrance in the model. If one dimer serves as the target and one monomer as the enzyme, the DC domain does not participate in the target interaction. The docking model is reasonable in terms of steric hindrance and the functioning of the DC domain only when a dimer acts as the enzyme and a monomer acts as the target.

One monomer is docked in the catalytic site of molecule B in the AaHIV dimer, during which the metalloproteinase active site of molecule B is leashed to the initial cleavage site of the monomer based on the structure of tripeptide binding to the zinc ion in the active site (Fig. 4A). The docking model shows that the C-domain of the target monomer is stretched to interact with the D-domain of molecule A from the dimer. The M-domain of the monomer interacts with the C-domain of molecule A and M-domain of molecule B, simultaneously presenting its cleavage site to the catalytic site of molecule B (Fig. 4A). In this model, the residues of HVR1 of molecule A are on the contact surface together with other residues such as residues 504–520, which contribute to target recognition. Simultaneously, the D-domain of molecule A participates in remote recognition of targets and adjustment of the substrate in the enzymatic center of molecule B. A different model is proposed based on the results of the docking experiment in which it is proposed that these proteins recognize their targets through the D-domain of molecule A from the dimer and hydrolyze them with the M-domain of molecule B (Fig. 4C). Similarly, ADAM1 can form dimer with ADAM2 [16] and the dimer may recognize their target proteins and hydrolyze them through the same mechanism as that of the autolytic process of AaHIV. This may represent a new model of target recognition and hydrolysis of ADAM family proteins.

ADAMs are widely distributed, and these enzymes proteolyze cell surface proteins to release functional peptides for many biological processes. Dysregulation of the functions of these proteins is also linked to different pathological states [22]. Investigation of the structural basis of autolysis of AaHIV suggested a new model in which the proteins form dimers, and one molecule offers the DC domain for adhesion while the other provides the M-domain for catalysis. These results may improve our understanding of target recognition and the processing mechanism of ADAMs.

Acknowledgments

We thank Meng Xu and Zheng Zhao for their assistance in structure docking. We also thank Yuhui Dong and Peng Liu at Beijing Synchrotron Radiation Factory for their support for data collection. This work was supported by Grants from the Chinese National Natural Science Foundation (30121001, 30025012, and 30571066), the Chinese Ministry of Science and Technology (2006CB806500 and 2006AA02A318), and the Chinese Academy of Sciences (KSCX1-YW-R-60).

Appendix A. Supplementary data

Supplementary data associated with this article can be found, in the online version, at doi:10.1016/j.bbrc.2009.06.004.

References

[1] J.B. Bjarnason, J.W. Fox, Hemorrhagic metalloproteinases from snake venoms, Pharmacol. Ther. 62 (1994) 325–372.

[2] J.W. Fox, S.M. Serrano, Structural considerations of the snake venom metalloproteinases, key members of the M12 reprolysin family of metalloproteinases, Toxicon 45 (2005) 969–985.
[3] L.A. Hite, L.G. Jia, J.B. Bjarnason, J.W. Fox, CDNA sequences for four snake venom metalloproteinases: structure, classification, and their relationship to mammalian reproductive proteins, Arch. Biochem. Biophys. 308 (1994) 182–191.
[4] S. Fujimura, K. Oshikawa, S. Terada, E. Kimoto, Primary structure and autoproteolysis of brevilysin H6 from the venom of *Gloydius halys brevicaudus*, J. Biochem. 128 (2000) 167–173.
[5] J.W. Fox, S.M. Serrano, Insights into and speculations about snake venom metalloproteinase (SVMP) synthesis, folding and disulfide bond formation and their contribution to venom complexity, FEBS J. 275 (2008) 3016–3030.
[6] R. Marques-Porto, I. Lebrun, D.C. Pimenta, Self-proteolysis regulation in the *Bothrops jararaca* venom: the metallopeptidases and their intrinsic peptidic inhibitor, Comp. Biochem. Physiol. C Toxicol. Pharmacol. 147 (2008) 424–433.
[7] J.M. Gutierrez, A. Rucavado, T. Escalante, C. Diaz, Hemorrhage induced by snake venom metalloproteinases: biochemical and biophysical mechanisms involved in microvessel damage, Toxicon 45 (2005) 997–1011.
[8] A.S. Kamiguti, C.R. Hay, R.D. Theakston, M. Zuzel, Insights into mechanism of haemorrhage caused by snake venom metaloproteinases, Toxicon 34 (1996) 627–642.
[9] D.F. Seals, S.A. Courtneidge, The ADAMs family of metalloproteases: multidomain proteins with multiple functions, Genes Dev. 17 (2003) 7–30.
[10] J.M. White, ADAMs: modulators of cell–cell and cell–matrix interactions, Curr. Opin. Cell Biol. 15 (2003) 598–606.
[11] S. Takeda, T. Igarashi, H. Mori, S. Araki, Crystal structures of VAP1 reveal ADAMs' MDC domain architecture and its unique C-shaped scaffold, EMBO J. 25 (2006) 2388–2396.
[12] T. Igarashi, S. Araki, S. Takeda, Crystal structures of catrocollastatin/VAP2B reveal a dynamic, modular architecture of ADAM/adamalysin/reprolysin family proteins, FEBS Lett. 581 (2007) 2416–2422.
[13] J.R. Muniz, A.L. Ambrosio, H.S. Selistre-de-Araujo, M.R. Cominetti, A.M. Mourada-Silva, G. Oliva, R.C. Garratt, D.H. Souza, The three-dimensional structure of bothropasin, the main hemorrhagic factor from *Bothrops jararaca* venom: insights for a new classification of snake venom metalloprotease subgroups, Toxicon 52 (2008) 807–816.
[14] Z. Zhu, W. Gong, X. Zhu, M. Teng, L. Niu, Purification, characterization and conformational analysis of a haemorrhagin from the venom of *Agkistrodon acutus*, Toxicon 35 (1997) 283–292.
[15] J. Zang, Z. Zhu, Y. Yu, M. Teng, L. Niu, Q. Huang, Q. Liu, Q. Hao, Purification, partial characterization and crystallization of Acucetin, a protein containing both disintegrin-like and cysteine-rich domains released by auto-proteolysis of a P-III-type metalloproteinase AaHIV from *Agkistrodon acutus* venom, Acta Crystallogr. D Biol. Crystallogr. 59 (2003) 2310–2312.
[16] C.P. Blobel, D.G. Myles, P. Primakoff, J.M. White, Proteolytic processing of a protein involved in sperm–egg fusion correlates with acquisition of fertilization competence, J. Cell Biol. 111 (1990) 69–78.
[17] W. Gong, X. Zhu, S. Liu, M. Teng, L. Niu, Crystal structures of acutolysin A, a three-disulfide hemorrhagic zinc metalloproteinase from the snake venom of *Agkistrodon acutus*, J. Mol. Biol. 283 (1998) 657–668.
[18] P. Orth et al., Crystal structure of the catalytic domain of human ADAM33, J. Mol. Biol. 335 (2004) 129–137.
[19] F.X. Gomis-Ruth, Structural aspects of the metzincin clan of metalloendopeptidases, Mol. Biotechnol. 24 (2003) 157–202.
[20] K.F. Huang, S.H. Chiou, T.P. Ko, A.H.J. Wang, Determinants of the inhibition of a *Taiwan habu* venom metalloproteinase by its endogenous inhibitors revealed by X-ray crystallography and synthetic inhibitor analogues, Eur. J. Biochem. 269 (2002) 3047–3056.
[21] Z. Lou, J. Hou, X. Liang, J. Chen, P. Qiu, Y. Liu, M. Li, Z. Rao, G. Yan, Crystal structure of a non-hemorrhagic fibrin(ogen)olytic metalloproteinase complexed with a novel natural tri-peptide inhibitor from venom of *Agkistrodon acutus*, J. Struct. Biol. 152 (2005) 195–203.
[22] D.R. Edwards, M.M. Handsley, C.J. Pennington, The ADAM metalloproteinases, Mol. Aspects Med. 29 (2008) 258–289.